PNAS
www.pnas.org

Supplementary Information for

Metabolic Stress Promotes Stop Codon Readthrough and Phenotypic Heterogeneity

Hong Zhang[a,1], Zhihui Lyu[a,1], Yongqiang Fan[b,c,d,1], Christopher R. Evans[b,1], Karl W. Barber[e,f], Kinshuk Banerjee[g], Oleg A. Igoshin[g,h], Jesse Rinehart[e,f], Jiqiang Ling[a,2]

[a]Department of Cell Biology and Molecular Genetics, The University of Maryland, College Park, MD 20742, USA
[b]Department of Microbiology and Molecular Genetics, McGovern Medical School, University of Texas Health Science Center, Houston, TX 77030, USA
[c]College of Life and Health Sciences, Northeastern University, Shenyang 110819, People's Republic of China
[d]Shenyang National Laboratory for Materials Science, Northeastern University, Shenyang 110819, People's Republic of China
[e]Department of Cellular & Molecular Physiology, Yale University, New Haven, CT 06520, USA.
[f]Systems Biology Institute, Yale University, New Haven, CT 06520, USA.
[g]Center for Theoretical Biological Physics, Rice University, Houston, TX 77005, USA
[h]Department of Bioengineering, Rice University, Houston, TX 77005, USA

[1]These authors contributed equally to this work
[2]Correspondence should be addressed to:
Jiqiang Ling: +1 (301) 405-1035; Email: jling12@umd.edu

This PDF file includes:

Supplementary Information Text
Figures S1 to S8
Tables S1 to S2
Legends for Movies S1 to S2
Legends for Datasets S1
SI References

Other supplementary materials for this manuscript include the following:

Movies S1 to S2
Dataset S1

Supplementary Information Text

Methods

Determining readthrough and frameshift rates. Stop codon readthrough and frameshift rates were determined as described (1). Briefly, *E. coli* cultures were incubated at 37 °C in a microplate reader (Synergy HTX, BioTek) using 96-well black side plates (Corning). The signals of mCherry, YFP, and A600 were measured every 20 minutes with spectrometry. To calculate translational error rates, the YFP/mCherry ratio of mCherry-TGA-YFP, mCherry-TAG-YFP, mCherry-TAA-YFP, mCherry-YFP +1 fs, and mCherry-YFP -1 fs was normalized by the YFP/mCherry ratio of the control mCherry-YFP reporter. The sequence of the +1 fs site is: ACCGGTGGCATGGATGAGCTGTACAAA**TAAA**CTGCAGACC; the sequence of the -1 fs site is: ACCGGTGGCATGGATGAGCTGTACAAA**TA**CTGCAGACC. The sequence of the *prfB* +1 fs reporter is: GGCCGCCAAAGCGGCCGCActtaggggtat**ctttga**ctacGGTACCCTCAGCAA AGGTGAA, with the lower-case letters indicate the *prfB* +1 fs site.

Determine intracellular pH. Intracelluar pH of *E. coli* cells were determined using the standard dye 2',7'-Bis-(2-Carboxyethyl)-5-(and-6)-Carboxyfluorescein, Acetoxymethyl Ester (BCECF-AM, Invitrogen) according to manufacturer's protocol. BCECF-AM is widely used to determine intracellular pH of bacteria (2-4). MG1655 cells were grown in LB or LB with 1% glucose at 37 °C. At each time point, 20 μM BCECF-AM was added to cultures for 60 min. The standard curve used MG1655 cells resuspended in 100 mM phosphate buffer with 20 mM sodium benzoate, which produces membrane permeable acid and equilibrates intracellular and media pH. The fluorescence was measured with excitation wavelengths of 420/50 nm (pH insensitive) or 485/20 nm (pH sensitive) and emission wavelengths of 520/20 nm. The ratio of 485 over 420 was calculated and plotted in SI Appendix, Fig. S1C.

Quantitative reverse transcription-PCR. Overnight cultures of *E. coli* strains were diluted 1:100 and grown in LB with or without 1% glucose at 37 °C for 5 h. The bacterial cells were then collected. Total RNA was extracted using the hot phenol method and residual chromosomal DNA was removed as described previously (5). Reverse transcription and PCR were performed using the iScript cDNA Synthesis Kit (Bio-Rad, Hercules, CA, USA) and GreenLink™ QPCR Master-Mix (BioLink Laboratories, San Diego, CA, USA) according to the manufacturers' instructions. All sample reactions were performed in triplicate, with *rrsA* gene used as an internal standard. The comparative Ct method was used to calculate the fold changes of target genes in samples grown with 1% glucose relative to samples grown without 1% glucose.

Mathematical modeling. Theoretical modeling of the variation of UGA readthrough with pH changes is based on the network shown in Fig. 2D. E represents the ribosome with UGA mRNA codon in the A-site, ER represents the RF2-bound state that undergoes a conformational transition to state ER*, and P_R is the state generated after RF2-induced hydrolysis of the peptide chain in the ribosome P-site (6). Et represents the aa-tRNA bound state, and the initial bound state Et undergoes GTP-hydrolysis to Et*. The pH-dependence of the rate of RF2-induced peptide hydrolysis is modeled by taking the catalysis rate constant $k_{p,R}$ as a function of pH based on a recent study (6). It is also shown that the peptide chain elongation in the presence of aa-tRNA does not involve any significant acid-base catalysis (7). Thus, we take the rates of the aa-tRNA (t) pathway to be pH-independent.

We study the kinetics of the whole network using the standard tools of first-passage technique (8). The probability to reach a given end-state (P_R or P_t) before the other starting from state-E is called the splitting probability (8). The UGA readthrough error η is defined as the ratio of the splitting probability of reaching the wrong end (P_t) to that of reaching the right end (P_R). The parameters to generate the trends of pH dependence are given in Table S2. The parameter choice for RF2 with a pH-dependent catalytic rate constant $k_{p,R}$ (pH) is based on the recent study of Indrisiunaite *et al.* (6) that gives a catalytic rate of ~22 s^{-1} for RF2-induced peptide hydrolysis at pH 7.5. The error rises with decreasing pH (Fig. 2D)

with a steeper slope below pH ~6.0. The η vs. pH curve gives an error ~2% at pH 7.5 and ~8% near pH 5.0.

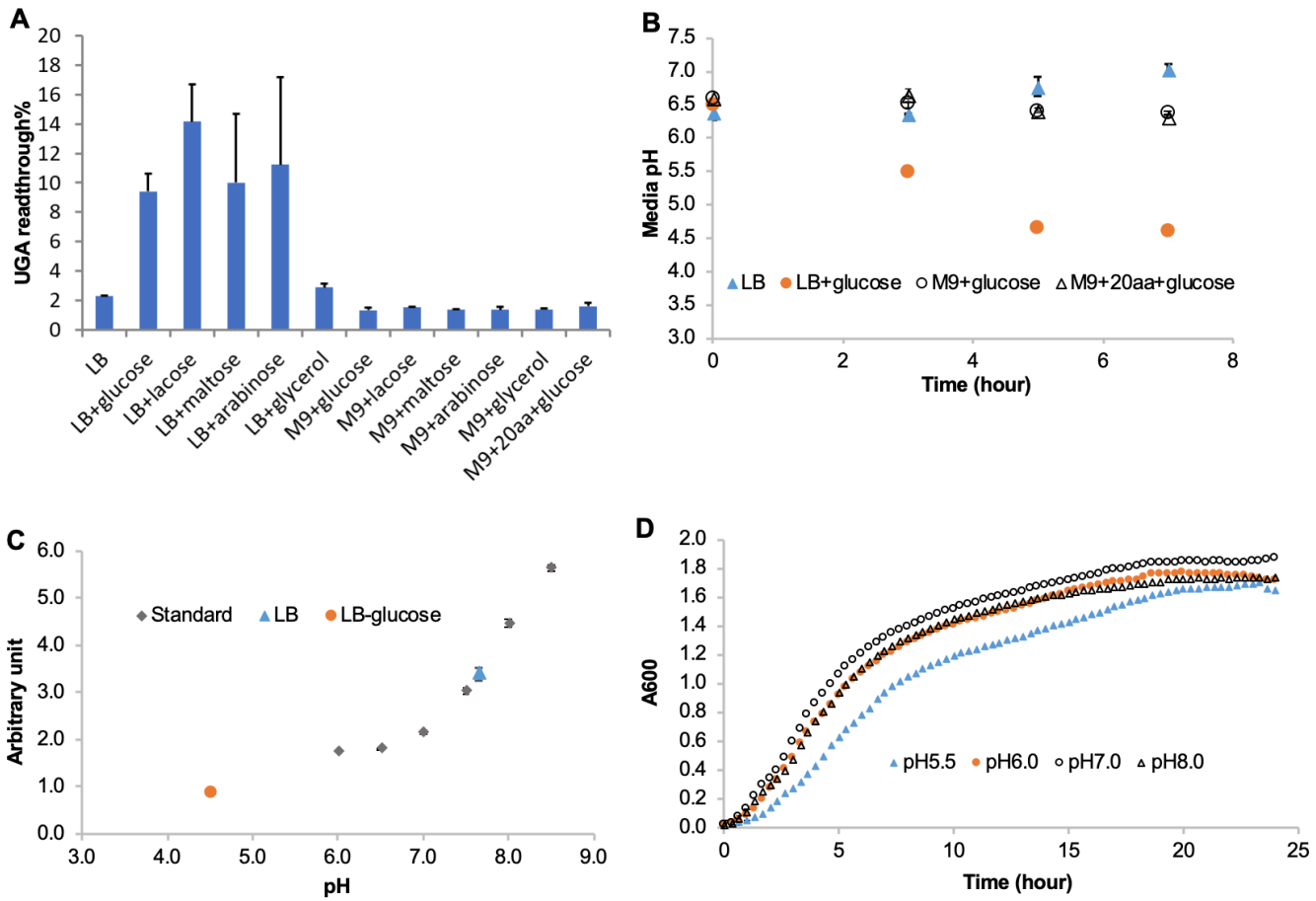

Fig. S1. UGA readthrough and pH in various media. (*A*) *E. coli* MG1655 cells carrying mCherry-TGA-YFP were grown in media with different carbon sources for 24 h, and the UGA readthrough level was determined with a plate reader as in Fig. 1. Addition of sugar in LB increased the level of UGA readthrough in the bacterial population. (*B*) Media pH of MG1655 cultures. (*C*) Intracellular pH of MG1655 at 5 h determined with BCECF-AM. Phosphate buffer with sodium benzoate at different pH was used as standard. (*D*) Representative growth curve of MG1655 in phosphate buffered LB at various pH. Error bars represent one standard deviation (n = 3).

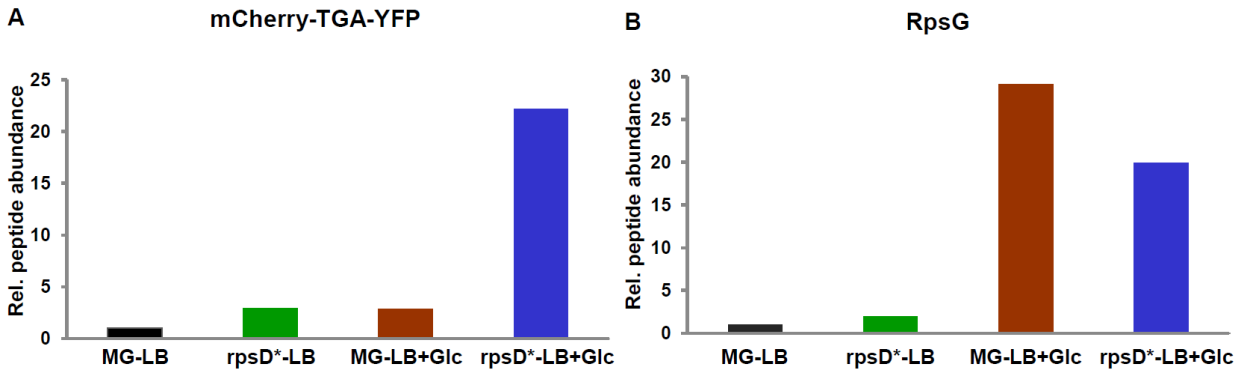

Fig. S2. Quantitative mass spectrometry confirms that excess carbon increases the level of UGA readthrough. Label-free mass spectrometry results of cells grown in LB glucose from Fig. 1D were compared with those of cells grown in LB (1). The peak area of **W**LQTSAGEAAAK (mCherry-TGA-YFP) or QPALGYLN**W**TPK (RpsG) in MG1655 grown in LB was set to 1. For both the mCherry-TGA-YFP reporter and RpsG, the *rpsD** mutation and excess glucose increased the levels of peptides resulting from UGA suppression by Trp.

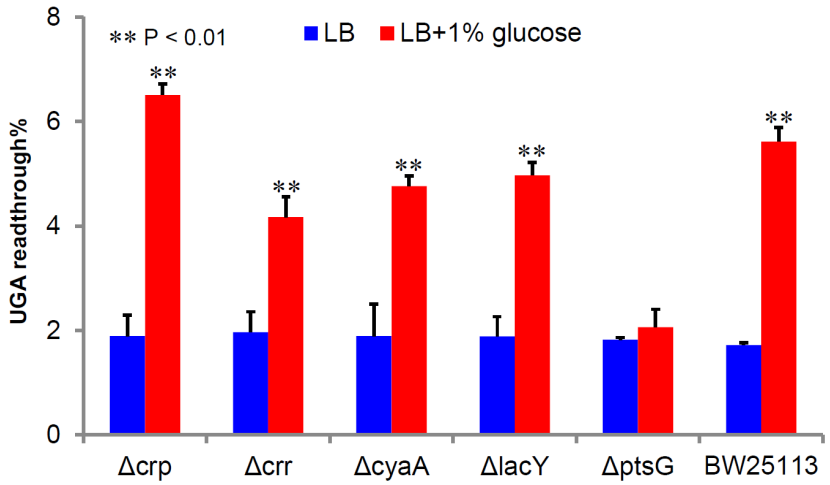

Fig. S3. Increased UGA readthrough depends on glucose uptake but not the cAMP-CRP pathway. Strains used here were from the Keio knockout *E. coli* library with the parental strain BW25113 (9). *crp* encodes cyclic AMP (cAMP) receptor protein, which regulates multiple metabolic pathways (10); cAMP synthesis is controlled by phosphorylated glucose that activates the adenylate cyclase CyaA; Crr catalyzes phosphorylation of glucose; LacY is a transporter of lactose inhibited by phosphorylated glucose; and PtsG mediates glucose uptake (10). Error bars represent one standard deviation (n = 3). P values were determined using unpaired *t* test.

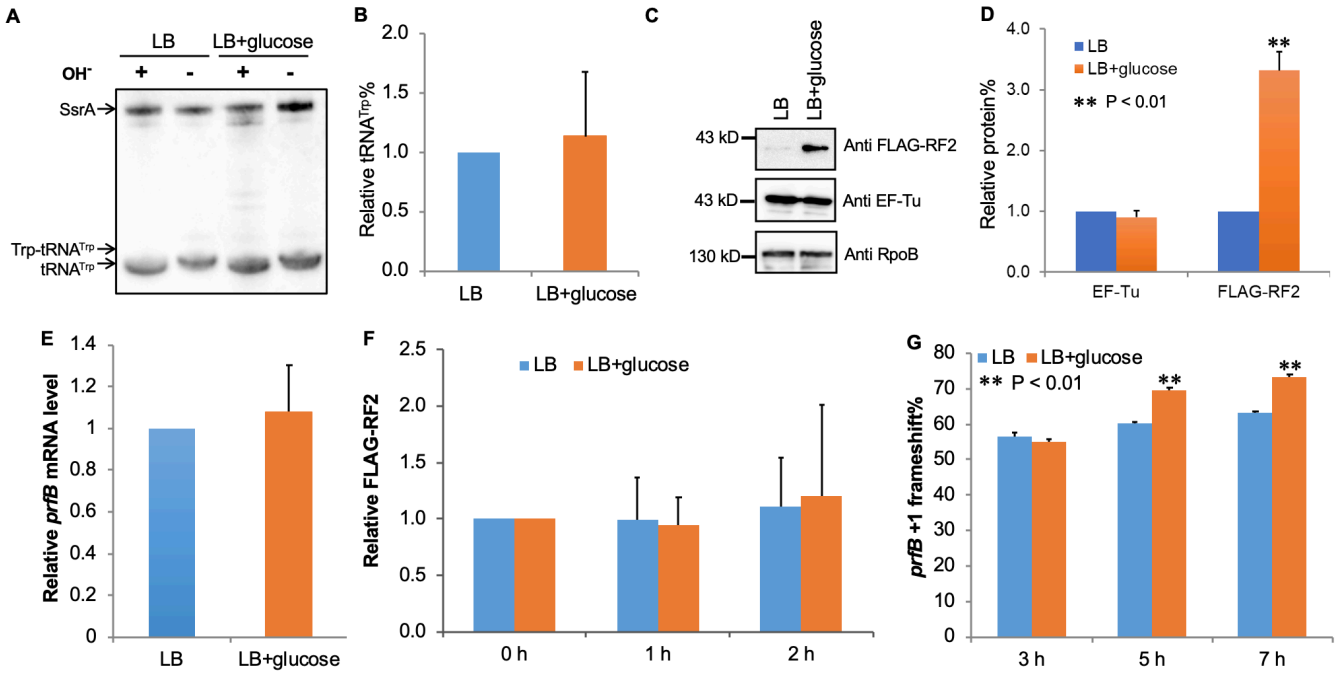

Fig. S4. Effects of glucose on expression of tRNA^{Trp}, EF-Tu, and RF2. MG1655 cells were grown in LB or LB with 1% glucose. (*A*, *B*) Acidic gel northern blotting of total RNAs isolated from *E. coli* cells with or without alkaline treatment to deacylate aminoacyl-tRNAs. Probes for tRNA^{Trp} and the control SsrA were used for blotting. No significant change in the levels of tRNA^{Trp} or Trp-tRNA^{Trp} were observed between cells grown in LB and LB glucose. (*C*, *D*) Western blotting of MG1655 derivative cells (with a FLAG tag at the C terminus RF2) grown in LB and LB glucose. (*E*) Relative levels of *prfB* mRNA determined by qRT-PCR. (*F*) Degradation time course of FLAG-RF2 protein in MG1655 grown in LB or LB+glucose for 5 h. Protein synthesis was stopped by addition of 100 μg/ml chloramphenicol and cell extracts were prepared after 0, 1 and 2 h. The levels of FLAG-RF2 were determined with Western blotting at each time point, with the level at 0 h set to 1. (*G*) Levels of *prfB* +1 frameshift determined with an *mCherry-prfB* +1-*yfp* reporter. Error bars represent one standard deviation (n ≥ 3). P values were determined using unpaired *t* test.

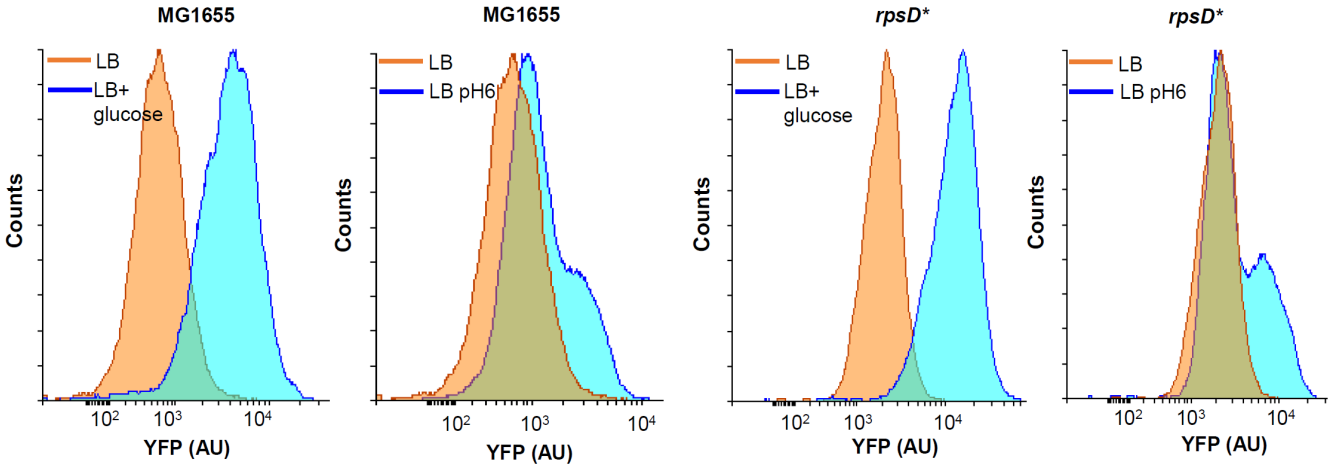

Fig. S5. Flow cytometry reveals that excess glucose and low pH increase UGA readthrough. MG1655 and *rpsD** cells carrying eCFP-TGA-YFP were grown in LB or LB with 1% glucose for 24 h, and subjected to flow cytometry analyses. The YFP signal resulting from UGA readthrough increased upon addition of glucose or at pH6. n = 10000.

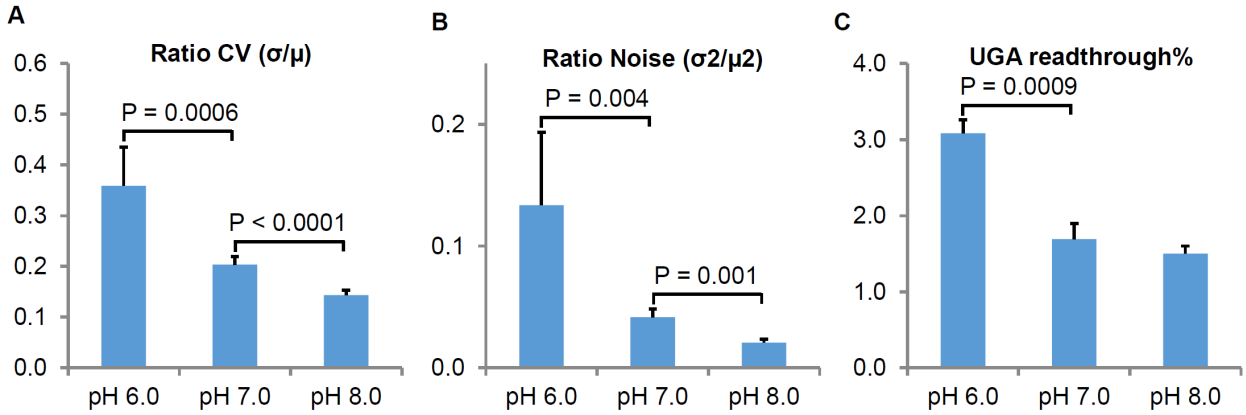

Fig. S6. Lowering pH increases the heterogeneity of UGA readthrough. MG1655 cells were grown at LB with different pH for 24 h, and analyzed with fluorescence microscopy (*A*, *B*) or plate reader (C) as in Figs. 1 and 3. Lowering pH increases both the level and noise of UGA readthrough. Error bars represent one standard deviation (n ≥ 3). P values were determined using unpaired *t* test.

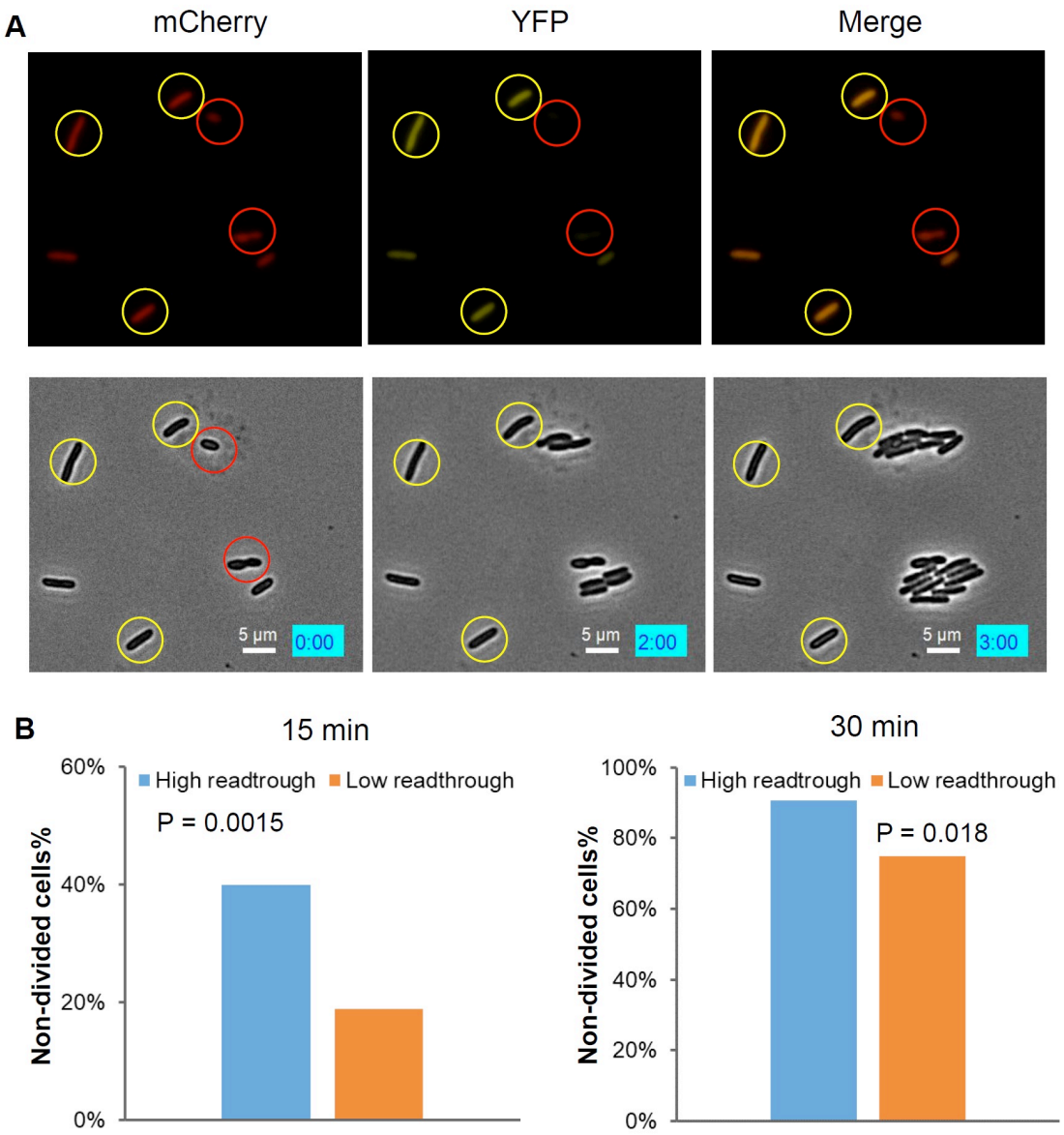

Fig. S7. Single cells with high UGA readthrough are more sensitive to streptomycin. MG1655 cells carrying the mCherry-TGA-YFP reporter were grown in LB with 1% glucose for 24 h before treatment with 20 μg/ml streptomycin for 15 or 30 min. Cells were then placed on LB agar pad for time-lapse microscopy as in Fig. 4. (*A*) Microscopy images showing individual cells with fluorescence (top) and phase contrast (bottom). Cells with high and low UGA readthrough were indicated with yellow and red circles. (B) Percentage of non-divided cells at 3 h in high and low readthrough groups. The P value was determined using the Chi-Square test (n = 214 and 164 for 15 and 30 min samples, respectively).

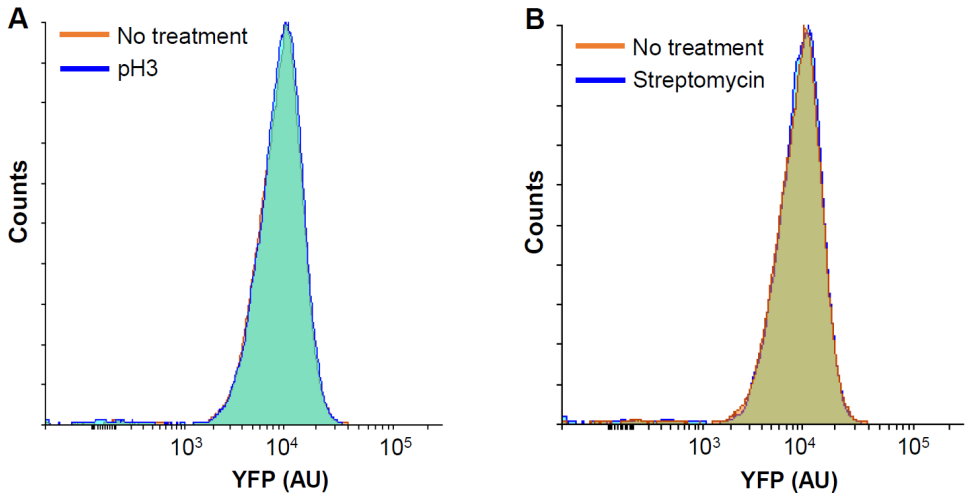

Fig. S8. Flow cytometry reveals that excess glucose and low pH increase UGA readthrough. MG1655 cells were grown in LB with 1% glucose for 24 h and treated with LB pH3 or 20 μg/ml streptomycin for 30 min. Samples were taken before and after the treatment for flow cytometry analyses. Neither acid or streptomycin treatment for 30 min altered the level or distribution of UGA readthrough among the individual cells.

Table S1. Identified peptides resulting from UGA readthrough in LB with glucose.

Sample[1]	Gene ID	Sequence
MG1655 m-TGA-y	*yjjA*	QGLNFISCTAK
MG1655 m-TGA-y	REPORTER	CLQTSAGEAAAK
MG1655 m-TGA-y	REPORTER	DHMVLLEFVTAAGITHGMDELYK
MG1655 m-TGA-y	REPORTER	EDGNILGHK
MG1655 m-TGA-y	REPORTER	FEGDTLVNR
MG1655 m-TGA-y	REPORTER	FSVSGEGEGDATYGK
MG1655 m-TGA-y	REPORTER	GEELFTGVVPILVELDGDVNGHK
MG1655 m-TGA-y	REPORTER	LEYNYNSHNVYITADK
MG1655 m-TGA-y	REPORTER	LICTTGK
MG1655 m-TGA-y	REPORTER	SAMPEGYVQER
MG1655 m-TGA-y	REPORTER	WLQTSAGEAAAK
MG1655 m-TGA-y	*rpsG*	QPALGYLNWTPK
MG1655	*yjjA*	QGLNFISCTAK
MG1655	*ribB*	ASWKPLLNLLP
MG1655	*rpsG*	QPALGYLNWTPK
*rpsD** m-TGA-y	*yjjA*	QGLNFISCTAK
*rpsD** m-TGA-y	REPORTER	AAAGTMSK
*rpsD** m-TGA-y	REPORTER	DHMVLLEFVTAAGITHGMDELYK
*rpsD** m-TGA-y	REPORTER	EDGNILGHK
*rpsD** m-TGA-y	REPORTER	FEGDTLVNR
*rpsD** m-TGA-y	REPORTER	FSVSGEGEGDATYGK
*rpsD** m-TGA-y	REPORTER	GEELFTGVVPILVELDGDVNGHK
*rpsD** m-TGA-y	REPORTER	LEYNYNSHNVYITADK
*rpsD** m-TGA-y	REPORTER	QHDFFK
*rpsD** m-TGA-y	REPORTER	RDHMVLLEFVTAAGITHGMDELYK
*rpsD** m-TGA-y	REPORTER	SAMPEGYVQER
*rpsD** m-TGA-y	REPORTER	WLQTSAGEAAAK
*rpsD** m-TGA-y	*mngB*	LAGIAIK
*rpsD** m-TGA-y	*phnJ*	KNQPINR
*rpsD** m-TGA-y	*ydgU*	RFYLSR
*rpsD** m-TGA-y	*nrfC*	YGEVSQVR
*rpsD** m-TGA-y	*ribB*	ASWKPLLNLLP
*rpsD**	*yjjA*	QGLNFISCTAK
*rpsD**	*ribB*	ASWKPLLNLLP
*rpsD**	*rpsG*	QPALGYLNWTPK

[1] MG1655 or *rpsD** cells with or without the UGA readthrough reporter (m-TGA-y) were grown in LB + 1% glucose for 24 hours, collected, and prepared for mass spectrometry.

Table S2. Parameter values to fit the pH Dependence of UGA readthrough

Parameter	Value
$k_{1,R}$	300 $M^{-1}s^{-1}$
$k_{-1,R}$	2 s^{-1}
$k_{2,R}$	175 s^{-1}
$k_{-2,R}$	75 s^{-1}
$k_{1,t}$	75 $M^{-1}s^{-1}$
$k_{-1,t}$	1.5 s^{-1}
$k_{2,t}$	5.6 s^{-1}
$k_{3,t}$	0.12 s^{-1}
$k_{p,t}$	0.07 s^{-1}

The parameter choice were based on the references (6, 11).

Movie S1. Time-lapse microscopy of MG1655 grown in LB glucose and treated with pH3. See PNAS_202013543_s2.avi. Linked to Fig. 4A.

Movie S2. Time-lapse microscopy of MG1655 grown in LB glucose and treated with streptomycin. See PNAS_202013543_s3.avi. Linked to Fig. S7A.

Dataset S1. Complete characterization of peptides resulting from UGA readthrough in LB with glucose (see supplemental Excel file).

SI References

1. Y. Fan *et al.*, Heterogeneity of stop codon readthrough in single bacterial cells and implications for population fitness. *Mol Cell* **67**, 826-836 (2017).
2. J. Choi, E. A. Groisman, Acidic pH sensing in the bacterial cytoplasm is required for Salmonella virulence. *Mol Microbiol* **101**, 1024-1038 (2016).
3. S. Chakraborty, H. Mizusaki, L. J. Kenney, A FRET-based DNA biosensor tracks OmpR-dependent acidification of Salmonella during macrophage infection. *PLoS Biol* **13**, e1002116 (2015).
4. S. Okutani *et al.*, Mechanical damage to Escherichia coli cells in a model of amino-acid crystal fermentation. *J Biosci Bioeng* **113**, 487-490 (2012).
5. E. Masse, C. K. Vanderpool, S. Gottesman, Effect of RyhB small RNA on global iron use in *Escherichia coli*. *J Bacteriol* **187**, 6962-6971 (2005).
6. G. Indrisiunaite, M. Y. Pavlov, V. Heurgue-Hamard, M. Ehrenberg, On the pH dependence of class-1 RF-dependent termination of mRNA translation. *J Mol Biol* **427**, 1848-1860 (2015).
7. P. Bieling, M. Beringer, S. Adio, M. V. Rodnina, Peptide bond formation does not involve acid-base catalysis by ribosomal residues. *Nat Struct Mol Biol* **13**, 423-428 (2006).
8. N. G. v. Kampen, *Stochastic Processes in Physics and Chemistry* (North Holland, 2007).
9. T. Baba *et al.*, Construction of *Escherichia coli* K-12 in-frame, single-gene knockout mutants: the Keio collection. *Mol Syst Biol* **2**, 2006.0008 (2006).
10. J. Deutscher, C. Francke, P. W. Postma, How phosphotransferase system-related protein phosphorylation regulates carbohydrate metabolism in bacteria. *Microbiol Mol Biol Rev* **70**, 939-1031 (2006).
11. L. Cochella, R. Green, An active role for tRNA in decoding beyond codon:anticodon pairing. *Science* **308**, 1178-1180 (2005).